# Superlattice Microrefrigerators Fusion Bonded With Optoelectronic Devices

Yan Zhang, Gehong Zeng, Joachim Piprek, Avram Bar-Cohen, *Fellow, IEEE*, and Ali Shakouri

***Abstract*—A three-dimensional (3-D) electrothermal model was developed to study the InP-based thin-film $In_{0.53}Ga_{0.47}As/In_{0.52}Al_{0.48}As$ superlattice (SL) microrefrigerators for various device sizes, ranging from $40 \times 40$ to $120 \times 120$ $\mu$m $^2$. We discussed both the maximum cooling and cooling power densities (CPDs) for experimental devices, analyzed their nonidealities, and proposed an optimized structure. The simulation results demonstrated that the experimental devices with an optimized structure can achieve a maximum cooling of 3 °C, or equivalently, a CPD over 300 W/cm$^2$. Furthermore, we found it was possible to achieve a maximum cooling of over 10 °C; equivalently, a CPD over 900 W/cm$^2$, when the figure of merit ($ZT$) of InGaAs/InAlAs SL was enhanced five times with nonconserved lateral momentum structures. Besides monolithic growth, we also proposed a fusion bonding scheme to simply bond the microrefrigerator chip on the back of the hot spots, defined as two-chip integration model in this paper. The cooling effect of this model was analyzed using ANSYS simulations.**

***Index Terms*—Cooling power density (CPD), electrothermal simulation, integration, maximum cooling, microrefrigerators, superlattice (SL), thermionic, thermoelectric (TE).**

## NOMENCLATURE

| | |
|---|---|
| SL | Superlattice, a periodic multilayer which is synthetic and where a unit cell, consisting of successive layers that are chemically different from their adjacent neighbors, is repeated. |
| WDM | Wavelength-division-multiplexing, a fiberoptic transmission technique that employs different light wavelengths to transmit data in parallel channels. |
| HIT | Heterostructure integrated thermionic, integrated cooling of devices using thermionic emission in semiconductor heterostrucutres. |
| Cooling | Temperature, "cools down" from ambient (25 °C). |
| CPD | Cooling power density, W/cm$^2$. |
| $ZT$ | Figure of merit, no unit. |
| TE | Thermoelectric. |
| COP | Coefficient of performance. |
| S | Seebeck coefficient, $\mu$V/K. |
| $\sigma$ | Electrical conductivity, $(\Omega\cdot\text{cm})^{-1}$. |
| k | Thermal conductivity, W/mK. |
| $\Delta$ T | Temperature difference, K or °C. |
| $T_{\max}$ | Maximum cooling temperature, K or °C. |
| $T_S$ | Heatsink temperature, K or °C. |
| $T_{\rm c}$ | Cold side temperature, K or°C. |
| $\Delta Q$ | Effective interface heating/cooling power, W. |
| I | Supplied current to microrefrigerator, mA. |
| $Q_{\rm c}$ | Cooling power, W. |
| $\chi$ | Percentage of Joule heating flowing back to the cold surface, no unit. |
| $R_{\rm e}$ | Electrical resistance, $\Omega$. |
| $R_{\rm th}$ | Thermal resistance, K/W. |

Manuscript received July 1, 2004; revised March 24, 2005. This work was supported by DRAPA HERETIC and NSF CAREER. This work was recommended for publication by Associate Editor B. Mack upon evaluation of the reviewers' comments.

Y. Zhang and A. Shakouri are with the Department of Electrical Engineering, University of California, Santa Cruz, CA 95064 USA (e-mail: ali@soe.ucsc.edu).

G. Zeng and J. Piprek are with the Electrical and Computer Engineering Department, University of California, Santa Barbara, CA 93106 USA.

A. Bar-Cohen is with the Department of Mechanical Engineering, University of Maryland, College Park, MD 20742 USA.

Digital Object Identifier 10.1109/TCAPT.2005.859747

## I. INTRODUCTION

CURRENT research trends in optoelectronic devices are moving toward increased speed, wavelength capacity, and level of integration. Lasers and optoelectronic devices are very sensitive to temperature. Heat flux in lasers' active region can reach up to kW/cm$^2$. The subsequent temperature rise can shift wavelength, reduce output power and decrease devices' lifetime [1]. The temperature-dependent wavelength shift is typically $\sim$ 0.1 nm/°C [2]. The channel spacing in WDM is only 0.2 $\sim$0.8 nm. Thus a few degrees temperature change can result in signal crosstalk and distortion. Currently, $Bi_2Te_3$ bulk thermoelectric (TE) coolers are being widely used in optoelectronics to realize temperature stabilization. However, their low efficiency, low cooling power density (CPD), and bulk size limit their applications [3]. Since the 1980s, thermal designers have been looking for cooling solutions that can be monolithically integrated with lasers.

In 1984, Hava *et al.* [4] observed a 2 °C temperature change on a GaAs/GaAlAs laser diode when it was monolithically integrated with an $n^+$ GaAs substrate TE elements at 6-A current. He concluded that the benefit of the improved cooling was due to heat spreading by metallic layer. However, the additional advantage of Peltier-effect cooling was minimized because of the relatively small ratio of Seebeck coefficient to thermal conductivity for $Ga_{1-x}Al_xAs$ alloys. In 1985, Dutta *et al.* [5] achieved a 2.5 °C temperature change on a InGaAsP laser diode when they monolithically integrated it with n–InP substrate TE elements at 50-mA current. In 1991, Berger *et al.* [6] reported a 7. 5 °C temperature change on a GaAs/AlGaAs vertical-cavity surface-emitting laser when they monolithically integrated their laser with $n^+$ GaAs substrate TE elements at 100-mA current. However, all these results were not convincing since there were no direct temperature measurement data, instead, the temperature changes were estimated by the wavelength shift of the light emitted from the laser diode. Both the temperature stability of the laser and accuracy of photoluminescence characterization could affect the temperature data. More importantly,

1521-3331/$20.00 © 2005 IEEE

in a three-terminal device geometry, the current sent to the substrate could affect the bias condition of the laser and thus its wavelength [7]. For example, the 7.5 °C temperature change reported by Berger *et al.* could be overestimated. According to the Peltier coefficient and resistivity data that they reported in the paper, we could calculate the maximum power factor ($S^2\sigma$), $1.45 \times 10^{-3}$ W/mK$^2$ for an n–GaAs with a doping concentration of $10^{17}$ cm$^{-3}$. Using the thermal conductivity data reported by Hava and Hunsperger [8] we calculated the figure of merit, $ZT = S^2\sigma$/k [9]. Now with the known $ZT$, we could estimate the maximum cooling temperature of this material in the ideal situation with the equation, $T_{\max} = (1/2)ZT_c^2$ [9]. It turned out that the material that Berger *et al.* used in his experiments could only achieve a maximum cooling temperature of 3.3 °C in an ideal situation. Considering contact resistance and other nonideal factors, the maximum cooling could be further diminished.

Conventional TE coolers are based on Peltier effect at metal–semiconductor junctions. When electrons flow from a material in which they have an average transport energy smaller than the Fermi energy to another material in which their average transport energy is higher, they absorb thermal energy from the lattice and this cools the junction between two materials. In our thin film device, we add in a SL layer between the metal and substrate. In the thermionic emission process, hot electrons from a cathode layer are selectively emitted over a barrier to the anode junction. Since the energy distribution of the emitted electrons is almost exclusively on one side of Fermi energy, when current flows, strong carrier-carrier, and carrier-lattice scatterings tend to restore the quasiequilibrium Fermi distribution in the cathode by absorbing energy from the lattice, and thus cooling the emitter junction. The phonon blocking SL strategy strives to reduce the material's thermal conductivity by modifying the number of phonon modes and phonon transport, while leaving the electrical conductivity unaltered. Recent experimental results show an estimated $ZT_{\text{ave}}$ of 2.5 at room temperature [10]–[12]. This would translate to a respectable maximum coefficient of performance (COP) between 2 and 3. In addition, the experimental results showed that even though the Si/SiGe SL structure has inherently lower $ZT$ values at room temperature, it could cool four times better than the bulk silicon material device and achieve cooling power densities exceeding 680 W/cm$^2$ [13].

Recently, the InP-based superlattice microrefrigerator experimentally demonstrated a maximum cooling up to 2.5 °C or equivalently a CPD ~100 W/cm$^2$ at room temperature [14]–[16]. The enhanced CPD was achieved by adding a few $\mu$ms of SL layer (InGaAs/InGaAsP). The SL can reduce the cross-plane thermal conductivity below that of the alloy, due to increased phonon scattering [17]. Furthermore, the SL layer acts as an energy filter in the thermionic emission process, thus enhancing the hot electron filtering. Zhang *et al.* [18] also fabricated $Al_{0.1}Ga_{0.9}As/Al_{0.2}Ga_{0.8}As$ n-type SL microrefrigerators, which cools 0.8 °C at 25 °C and 2 °C at 100 °C for a $60 \times 60$ $\mu$m $^2$ device. No CPD data was reported on their devices. All these results demonstrated a promising trend of introducing nanostructured material, such as SLs, quantum dots etc. in the TE field [19].

In this paper, we mainly discuss cooling properties, maximum cooling and CPDs, of InGaAs/InAlAs SL microrefrigerators using three-dimensional (3-D) electrothermal models by ANSYS [20]. The modeling of the devices has been described in two parts: first, we studied the microrefrigerators model and analyzed all nonideal factors impact on its cooling; second part, we studied the potential of microrefrigerator in removing the hot spots in two-chip integration model (Section IV-C).

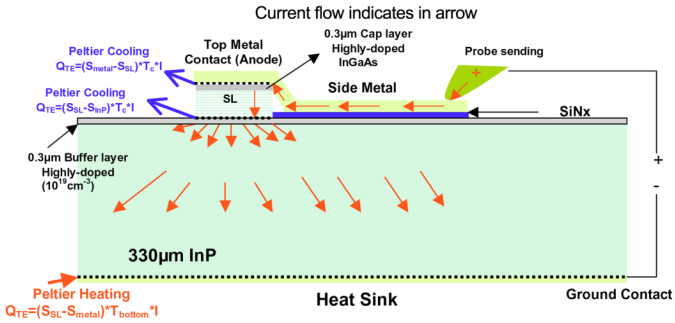


Fig. 1. Cross section view of the device geometry. (For best illustration, the drawing is not to scale. Current flow and effective thermoelectric cooling effects are indicated.) (Color version available online at http://ieeexplore.ieee.org.)

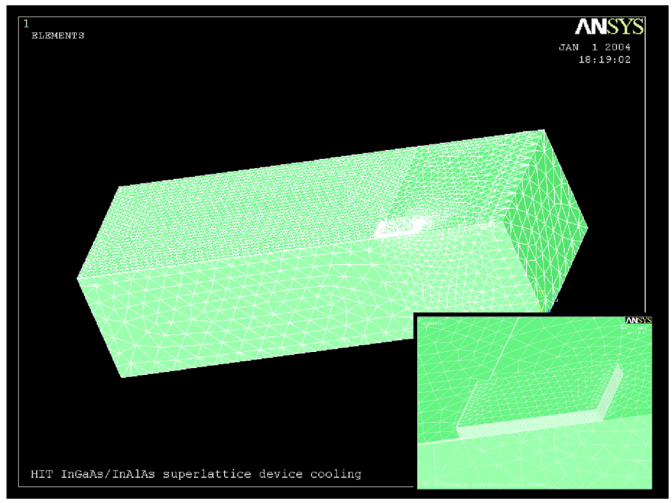


Fig. 2. HIT microrefrigerator with fine meshing in 3-D electrothermal model, right corner enlarged picture to illustrate the fine meshing in SL region. (Color version available online at http://ieeexplore.ieee.org.)

## II. Device Structure and 3-D Electrothermal Model

The heterostructure integrated thermionic (HIT) microrefrigerator consists of an $In_{0.53}Ga_{0.47}As/Al_{0.52}Ga_{0.48}As$ SL layer lattice matched to an n$^+$-InP substrate (330-$\mu$m-thick), and two highly doped ($10^{19}$ cm$^{-3}$) 0.3 $\mu$m-thick InGaAs layers, one underneath the SL used as buffer layer, and the other grown on top of the SL layer used as cap layer. The SL consists of 25 periods of 5nm thick InGaAs n-doped with silicon, with a doping concentration of $3 \times 10^{19}$ cm$^{-3}$ and 3-nm-thick undoped InAlAs. Superlattice structures were grown using molecular beam epitaxy (MBE). Devices were fabricated using conventional lithography, dry etching, and metallization techniques. Ni/AuGe/Ni/Au was used to make ohmic contacts to both cathode and anode. Fig. 1 shows a schematic cross section view of the device with the current flow and effective thermoelectric effects indicated. Fig. 2 shows the device structure with fine meshing in a 3-D electrothermal model.

TABLE I
MATERIALS PARAMETERS FOR InGaA/InAlAs SL MICROREFRIGERATOR

| **Thermal Conductivity** | | | | | | |
|---|---|---|---|---|---|---|
| Unit | Metal layer | SiNx | InP Substrate | Bottom Contact layer | SL Layer | Top Contact Layer |
| W/mK | 72 | 1 | 68 | 6.7 | 6.7 | 6.7 |
| **Resistivity** | | | | | | |
| Ohm-cm | 1.00e-05 | 1000 | 0.006 | 0.001 | 0.001 | 0.031 |
| **Seebeck coefficient Values (μV/K)** | | | | | | |
| $S_{metal}$ = 0; $S_{SL}$ = 130; $S_{InP}$ = 100; | | | | | | |

In our ANSYS model, the bulk Joule heating and heat conduction are automatically calculated by solving current continuity and heat conduction equations. We treat the thermionic-emission cooling process as effective interface cooling/heating effects, which are calculated in a linear transport region by the equation $\Delta Q = (S_1 - S_2)TI$ at both the metal–SL and SL–InP substrate. The cap layer is very thin (0.3 $\mu$m) and consist of highly-doped InGaAs alloy, thus the temperature gradient across this thin layer could be neglected. $S_1$ and $S_2$ are the effective Seebeck coefficients for materials on the two sides of the junctions: at the metal-SL interface, $S_1 = S_{\rm metal}, S_2 = S_{\rm SL}$ and at the SL-substrate interface, $S_1 = S_{\rm SL}, S_2 = S_{\rm InP}$. $T$ is the ambient temperature (25 °C = 298 K) and $I$ is the supplied current. Table I lists material properties that we used in the simulation. The cross-plane thermal conductivity of the SL was measured by Majumdar's group at UC Berkeley [21]. The Seebeck coefficient data was also experimentally measured [22]. A detailed description of the 3-D electrothermal model can be found in [23].

There are two methods we could use to integrate the microrefrigerators with optoelectronic devices. One is to monolithically grow the optoelectronic module on top of the microrefrigerator, which would take advantage of all the cooling that a single microrefrigerator could create. The second method is to attach the optoelectronic module and microrefrigerator together by fusion bonding, which is defined as two-chip integration model in this paper and illustrated in Fig. 3. In our model, we created a microrefrigerator chip and a 600 × 400 $\mu$m$^2$ optoelectronic chip. We attached the two modules together by eutectic bonding with a 3-$\mu$m gold interface and a 0.3 $\mu$m $SiN_x$ insulating layer preventing the current leaking from the microrefrigerator to the optoelectronic device or vice versa. At the target cooling area, the optoelectronic device's active region (hot spot), we applied heat flux to simulate the heat generated by the optoelectronic device operation. For convenient calculation, we made the hot spot size equal to the microrefrigerator device size.

## III. MAXIMUM COOLING AND CPD

The performance of the microrefrigerator was evaluated in terms of the maximum cooling temperature $\Delta T_{\rm max}$, the "cool down" from ambient (25 °C), and the CPD in all experiments and simulations below.

The maximum cooling we discuss in this paper refers to the temperature difference between the microrefrigerator top surface ($T_{\rm c}$) and the heatsink ($T_S$), which is equal to the ambient temperature, $\Delta T = T_S - T_{\rm c}$. To verify the simulation model, the maximum cooling for various device sizes were experimentally measured with two Omega E-type thermocouples, one on top of the microrefrigerator, and the other on top of the InP substrate, which was placed on the temperature controlled copper stage with thermal grease.

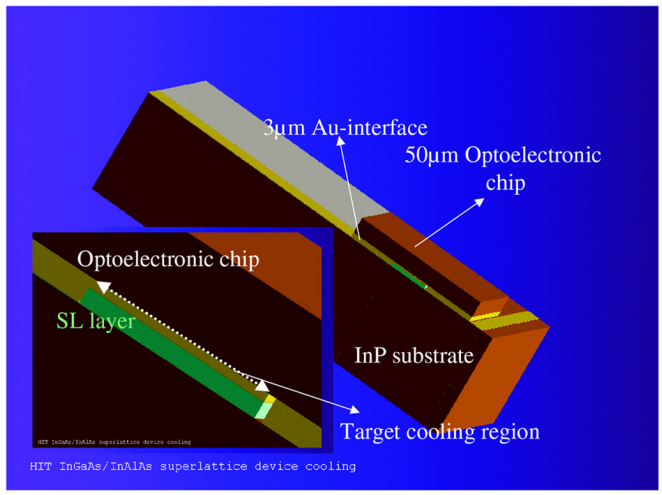


Fig. 3. Two-chip integration model of microrefrigerator with optoelectronic module. (Color version available online at http://ieeexplore.ieee.org.)

The cooling power was defined as the heat that the microrefrigerator could take at the point where maximum cooling equals zero. The heat conduction equation for microrefrigerators is similar to thermoelectric coolers, which is represented by: $Q_c = ST_cI - \chi I^2R_e - (\Delta T/R_{\rm th})$($Q_{\rm c}$ is the cooling power; $S$, seebeck coefficient; $T_{\rm c}$, cold side temperature; $I$, supplied current; $\chi$, percentage of Joule heating flowing back to the cold surface; $R_{\rm e}$ electrical resistance; $\Delta T$, temperature difference between hot and cold side; and $R_{\rm th}$, thermal resistance). When there is no heat applied on top of the microrefrigerator, $Q_{\rm c}$ =0, at an optimized current, the microrefrigerator reaches its maximum cooling. If we start to apply heat on top of the microrefrigerator, $Q_{\rm c}$ increases and $\Delta T$ decreases. When $\Delta T$ =0, the $Q_{\rm c}$ reaches the maximum value, which is defined as the maximum cooling power. The CPD equals the cooling power divide by the device area.

## IV. RESULTS AND DISCUSSION

### A. Microrefrigerator Device Cooling

In Fig. 4, we see a good correspondence between the simulations and experiments for all device sizes, which ensures the accuracy of the model. That different size devices have different cooling curves is due to geometry dependence of various nonideal parameters affecting the maximum cooling. For example,

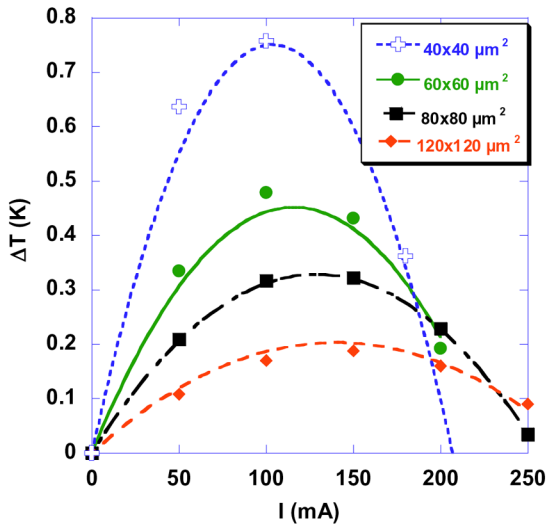


Fig. 4. Device cooling versus supplied current for various device sizes (individual dots are experimental measurement results, lines are simulated results). (Color version available online at http://ieeexplore.ieee.org.)

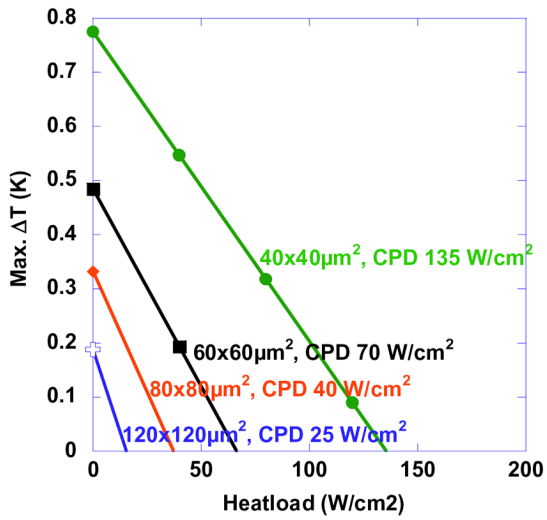


Fig. 5. Maximum cooling temperature versus applied heatload for various device sizes with CPDs indicated. (Color version available online at http://ieeexplore.ieee.org.)

contact resistance scales with area of the device while side contact resistance scales with square root of area. Similarly, SL and substrate electrical/thermal resistance have different area dependence. In the current device configuration, the optimized device size to achieve the best cooling is $40 \times 40$ $\mu$m $^2$, illustrated in Fig. 4. When the material properties or device structures change, the optimized size also changes. Furthermore, we also investigated the CPDs of these devices with the current model, as illustrated in Fig. 5. For current experimental devices, we could expect a CPD ranging from 25 to 135 W/cm$^2$ for device sizes ranging from $120 \times 120$ to $40 \times 40$ $\mu$m$^2$.

### *B. Improved Microrefrigrator Device Cooling*

From Figs. 4 and 5, we observe that the cooling of the device is only about 0.8 °C. From the calculations in the introduction, we know that the maximum cooling capacity of these devices is on the order of 3 °C–4 °C. Obviously, nonideal factors, Joule-heating and metal-semiconductor contact resistance, greatly diminish the maximum cooling of the device. The 3-D electrothermal model can be used to optimize the structure and reduce cooling loss due to these nonideal factors.

First, we try to find the optimized SL thickness and we found that the thicker SL, the higher cooling it achieved. Fig. 6 illustrates the maximum cooling that we could achieve if we increase the SL from 3 to 10 $\mu$m and keep all the other parameters the same. The maximum cooling of devices increases two times over the current device. The reason for this improvement is that we have a cascade of two TE elements (SL+substrate). Thicker SL increases the contribution of SL with respect to substrate, thus we got better cooling. However, the cooling performance is not monotonically increase with the SL thickness. When the SL gets thicker, its electrical resistance also gets higher. Thus, eventually, the increased Joule heating inside the SL will diminish the interface cooling. So there should be an optimized SL thickness to achieve the maximum cooling, but we did not observe this optimized value up to 10-$\mu$m thickness, which was also a practical SL thickness feasibly grown in the lab.

Second, we investigate the parasitic influence of metal-semiconductor contact resistance. From our experiences with

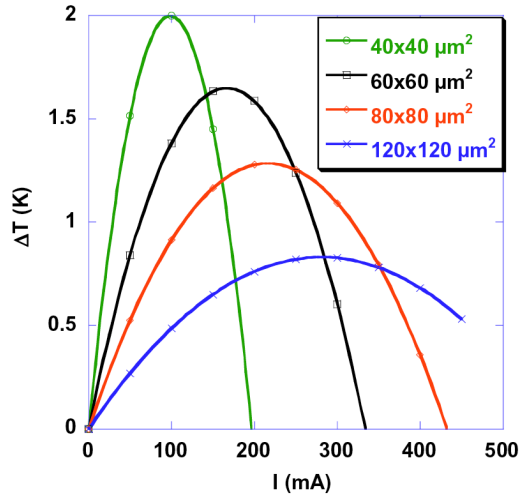


Fig. 6. Improved device (increasing SL to 10 $\mu$m thick) cooling versus supplied current. (Color version available online at http://ieeexplore.ieee.org.)

Si/SiGe SL microrefrigerator devices, we know this contact resistance is the bottleneck. For the Si/SiGe SL microrefrigerator, reducing this contact resistance, in theory the maximum cooling of microrefrigerator could be doubled (from 4.5 °C to 9 °C) [23]. However, it is interesting to find out that by reducing the metal-semiconductor contact resistance from $10^{-6}$ $\Omega$·cm$^{-2}$ to $10^{-8}$ $\Omega$·cm$^{-2}$ for these InGaAs/AlGaAs SL devices, we only see an improved cooling of $\sim 10\%$, as illustrated in Fig. 7.

Third, we also check the side contact resistance influence on the microrefrigerator cooling by reducing the side contact resistance to one tenth of its original value. Since the metal resistance and its thermal conductivity are directly related via Wiedemann–Franz law ($k/\sigma \sim$ constant), when we decrease the electrical resistivity of the side contact layer, we have to increase its thermal conductivity at the same time. The increased electrical conductivity results in less Joule heating, however, the increased contact probe thermal conductivity transfers heat more easily to the top of the microrefrigerator cooling region instead of spreading along the probe region and penetrating into the substrate. From Fig. 8, we find that the side contact resistance does not improve the cooling for small devices, but it almost doubles

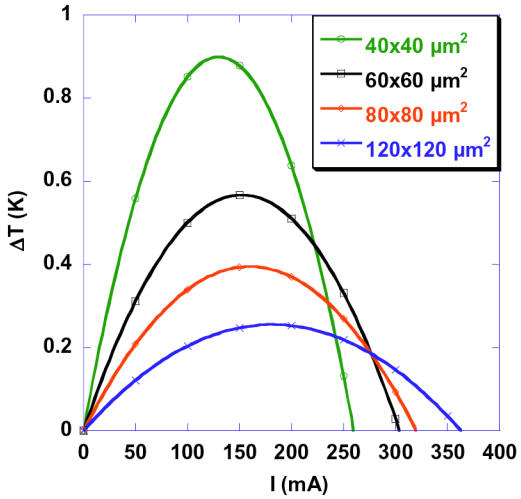


Fig. 7. Improved device (reducing the metal/semiconductor contact resistance) cooling versus supplied current. (Color version available online at http://ieeexplore.ieee.org.)

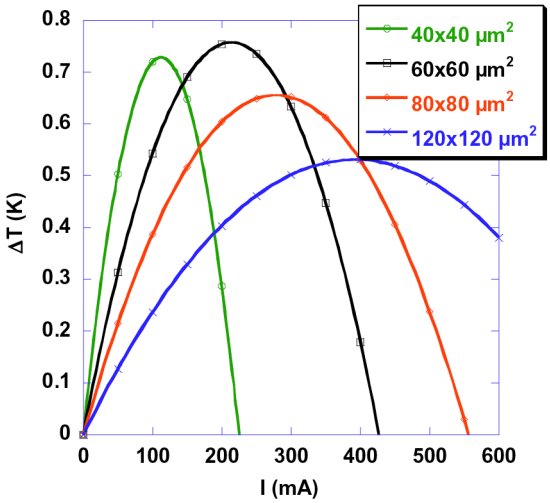


Fig. 8. Improved device (reducing side contact metal resistance) cooling versus supplied current. (Color version available online at http://ieeexplore.ieee.org.)

the cooling for the larger device, e.g., $120 \times 120\ \mu\text{m}^2$. This may be because large area devices require higher currents and thus there is more Joule heating in the side contact layer.

When we put the above three factors together, a thicker superlattice, lower metal contact resistance, and a lower side contact resistance, we get the overall optimized cooling effect, illustrated in Fig. 9. It is important to know that these three improvements could be all achieved by improving SL growth control and the device fabrication processes. With these improvements, the $40 \times 40\ \mu\text{m}^2$ devices achieved the maximum cooling of 3 °C at 150-mA supplied current, which is close to the material's theoretical limit 4 °C (obtained from the equation, $T_{\max} = (1/2)ZT_c^2$). The larger device, $120 \times 120\ \mu\text{m}^2$, maximum cools 1.5 °C at 600 mA. Besides the improvement in the maximum cooling temperature, the equivalent CPDs also increase significantly. The large CPD makes it promising to remove hot spots from very small local area into the big substrate. Fig. 10 illustrates the simulated CPDs as a function of device area for these optimized devices as compared with

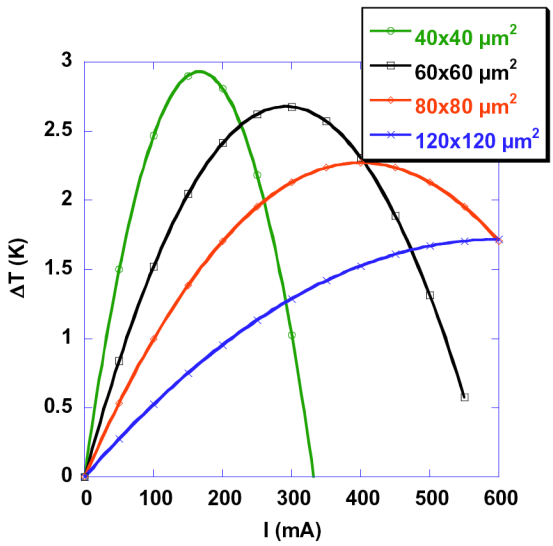


Fig. 9. Improved device (higher SL layer (10 $\mu$m), reduced metal/semiconductor contact and side metal contact resistance) cooling versus supplied current. (Color version available online at http://ieeexplore.ieee.org.)

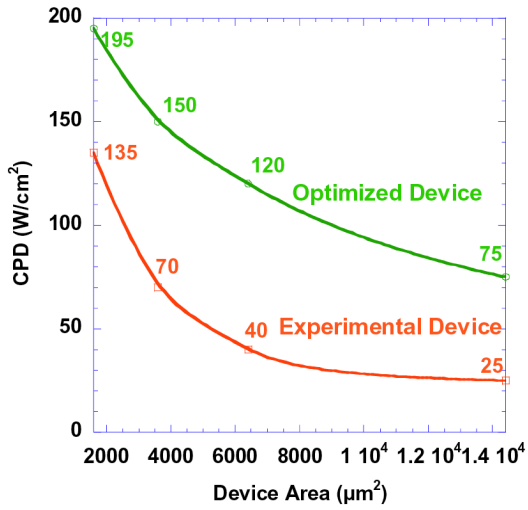


Fig. 10. CPDs versus device sizes for optimized SL devices as compared with the original devices. (Color version available online at http://ieeexplore.ieee.org.)

the original experimental devices. The CDP is increased by a factor of three for the $120 \times 120\ \mu\text{m}^2$ device by less than a factor of two for the $40 \times 40\ \mu\text{m}^2$ device. This nonmonotonic change will be investigated in future work.

Another parasitic nonideal factor that we could consider is the Joule heating from the substrate. Fig. 11 illustrates the maximum cooling that we could achieve if we remove the InP substrate and put the SL device directly on a copper plate. We noted that the cooling of the larger devices improves more significantly than the smaller devices when the substrate is removed. As illustrated in Fig. 11, the $120 \times 120\ \mu\text{m}^2$ device will have a comparable amount of cooling to a smaller device, like $40 \times 40\ \mu\text{m}^2$. The optimized device size is also shifted to $60 \times 60\ \mu\text{m}^2$ with a maximum cooling $\sim$4 °C. However, it requires more electrical power to reach the maximum cooling. These are all the factors that we need to consider while optimizing a device and applying them to hot spots.

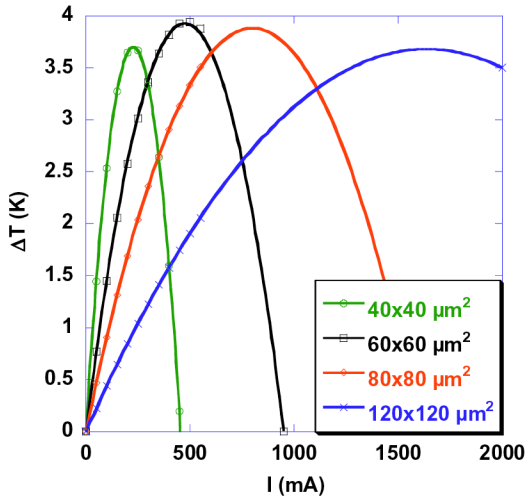


Fig. 11. Improved device cooling versus supplied current by removing InP substrate. (Color version available online at http://ieeexplore.ieee.org.)

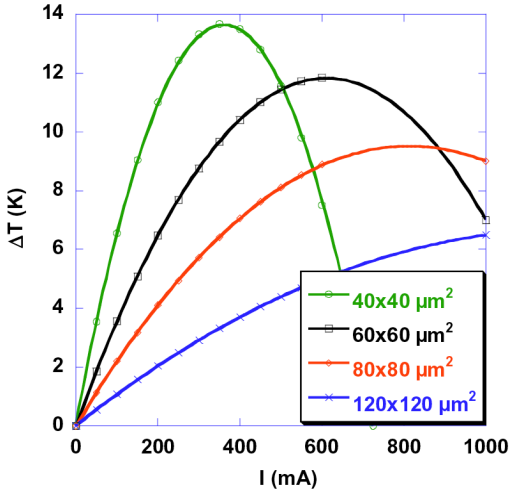


Fig. 12. Improved device (using nonconserved lateral momentum SL layer with higher doping) cooling versus current. (Color version available online at http://ieeexplore.ieee.org.)

However, all the results presented above do not reflect the limits of HIT microrefrigerator capabilities. According to the recent simulation results [24], [25], we could improve the device power factor five times if we could introduce the nonconserved lateral momentum with a higher doping in the SL layer. When the lateral momentum is conserved, only a limited number of hot electrons could be emitted above superlattice barriers. Only carriers with sufficiently large kinetic energy perpendicular to the barrier can pass over it and cool the emitter junction. However, if lateral momentum is not conserved, all the hot electrons could participate in thermionic emission and this will dramatically increase the maximum cooling. The nonconserved lateral momentum could be achieved by introducing embedded quantum dots and nonplanar barriers inside superlattice [26]. If we include the power factor improvement in our 3-D electrothermal model, it is interesting to find out that the small $40 \times 40$ $\mu$m$^2$ microrefrigerator cools up to $\sim$14 °C or an equivalent CPD exceeding 900 W/cm$^2$. Even the largest device $120 \times 120$ $\mu$m$^2$ achieves a maximum cooling of 6 °C or a CPD of 275 W/cm$^2$, as illustrated in Figs. 12 and 13.

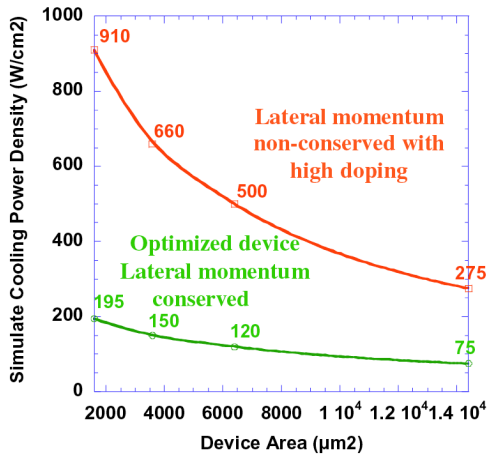


Fig. 13. CPD versus device size for non-conserved lateral momentum devices with higher doping compared with the original devices with optimized structure. (Color version available online at http://ieeexplore.ieee.org.)

It is important to note that a high COP is another advantage of microrefrigerators when compared with conventional TE coolers. For the experimental device, the maximum CPD achieved with only a minimal current of 0.1 A. The COP of these devices range from 0.3–0.6 for various device sizes $40 \times 40$–$120 \times 120$ $\mu$m$^2$. For the optimized device, with the nonconserved lateral momentum in the superlattice, the COP could be further improved. However, COP is also a strong function of current. The optimized current to achieve the maximum CPD is different from the current achieving the best COP. For example, the device, $40 \times 40$ $\mu$m$^2$, achieves its maximum CPD at 350 mA but maximum COP at 150 mA. Fig. 14 illustrates the COP versus current for the optimized devices assuming nonconserved lateral momentum.

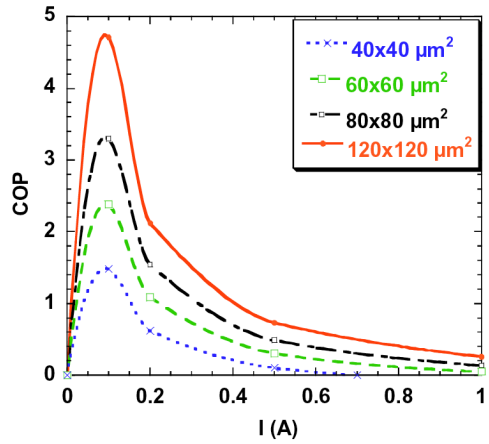


Fig. 14. COP versus supplied current for optimized devices assuming nonconserved lateral momentum in the superlattice. (Different curves representing different device sizes. (Color version available online at http://ieeexplore.ieee.org.)

### *C. Microrefrigerators' Potential in Removing Hot Spots in Two-Chip Integration Model*

The above sections discussed the cooling effects that we could achieve if we monolithically grow the laser structure directly on top of the microrefrigerator and if the current could be uniformly applied to the cooler device [27]. However, monolithic integration might be complicated considering all the growth conditions. Another option to utilize the microrefrigerator is to directly bond the optoelectronic chip on top of

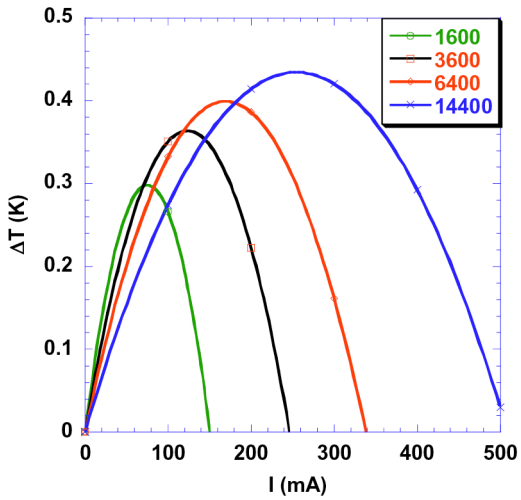


Fig. 15. Cooling at the targeted region (relative to ambient) in two-chip model with optimized device structures. (Color version available online at http://ieeexplore.ieee.org.)

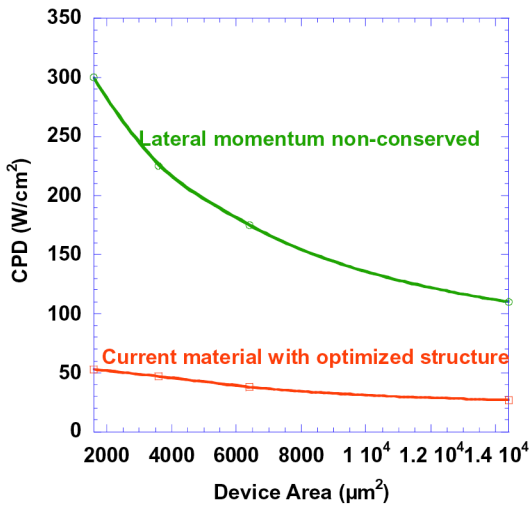


Fig. 16. CPDs versus device sizes with the optimized structure compared with nonconserved lateral momentum SL structure (Fig. 12). (Color version available online at http://ieeexplore.ieee.org.)

the microrefrigerator as two-chip integration model illustrated in Fig. 3. This model might not be the optimized integration method but we used it here to demonstrate a concept. From the maximum cooling and CPD results shown in Figs. 15 and 16, we notice that most of the cooling is lost in the interface layer. The optimized device model has a maximum cooling of 3 °C; however, it only cools 0.4 °C after integration with the optoelectronic module.

It is important to note that the temperature that we refer to here is the temperature "cool down," relative to ambient, which will be different from the relative temperature change during optoelectronic device operation. To demonstrate the difference, we illustrated the relative temperature difference between the two cases of cooler on and off during optoelectronic device operation in Fig. 17. In this figure, the simulated laser is: operating at 80 °C ambient temperature and convection coefficient is 1.27 W/cm$^2$ K (For fair comparison with results in Fig. 15, in this simulation, we assume all materials properties are constant as temperature change from 25 °C to 80 °C). When a hot spot (same size as microrefrigerator) is turned on by applying a heatflux of 300 W/cm$^2$, the hot spot region is heated up. At this time, when we turn on microrefrigerator by applying the optimized current, the hot spots temperature drops. The temperatures in Table II list the temperature at the hot spot region with hot spot and microrefrigerator off, and with hot spot on and microrefrigerator turning on with optimized current for various device sizes. The temperature difference between cooler on and off is four to five times larger than the temperature "cool down" from ambient, that we discussed earlier in this paper. It is important to note that this improvement is due to the fact that less amount of parasitic Joule heating could flow to the cold junction with different thermal boundary conditions for the overall chip. However, this improvement is not related with the additional convective thermal resistance. In this paper, mostly we choose the "cool down" temperature from ambient for easy comparisons to the cooling performance of the microrefrigerator alone before its integration. When analyzing a fully packaged device, the different boundary conditions could yield different cooling results, thus one has to analyze each case individually.

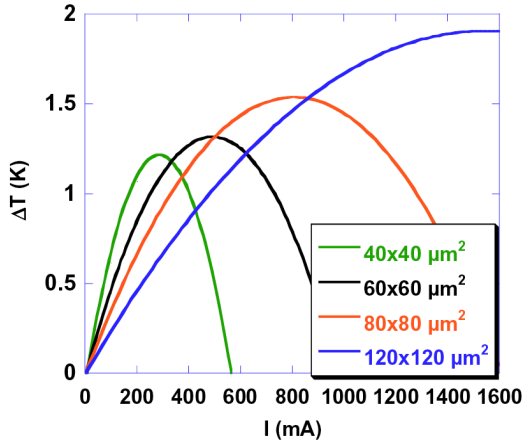


Fig. 17. Cooling of the optimized device (relative temperature difference compared to the case when microrefrigerator is off) versus supplied current. Here we assume different thermal boundary conditions for the package. (Color version available online at http://ieeexplore.ieee.org.)

We also observed that when we integrate the microrefrigerator with the optoelectronic module, the larger devices cool better than the smaller ones at the target-cooling region. This is opposite to the trend for individual microrefrigerators. Also, the CPDs reduced significantly after integration. For the optimized structure, the cooling power density reduces to ~50 W/cm$^2$ compared to the 200 W/cm$^2$ without an optoelectronic module, which means only one quarter of the cooling power is used effectively to cool the target region. We could improve the CPD to 910 W/cm$^2$ by using nonconserved lateral momentum SL samples, but this only provides 300 W/cm$^2$ at the target region in the two-chip model, where only one-third of the power is utilized. When we bond the microrefrigerator with the optoelectronic devices, there are many system issues that could be optimized. At this point, the low COP (or $ZT$ of the material) is not the main limiting factor. The more important factor is the additional thermal resistance from the integration. A more complete system level analysis on the integration of Si/SiGe SL microrefrigerators with microprocessors is studied elsewhere [28].

TABLE II
LISTED TEMPERATURES WHEN THE HOT SPOT ON WITH COOLER OFF AND HOT SPOT ON WITH COOLER ON FOR VARIOUS DEVICE SIZES

| Size (μm2) | hot spot T with cooler off ($^0$C) | substrate T($^0$C) | hot spot T with cooler on ($^0$C) | supplied I (mA) | ΔT (hot spot T wt cooler off - hot spot T wt cooler on) ($^0$C) |
|---|---|---|---|---|---|
| 1600 | 81.1 | 80 | 79.9 | 0.3 | 1.2 |
| 3600 | 81.6 | 80 | 80.3 | 0.5 | 1.3 |
| 6400 | 82 | 80 | 80.5 | 0.8 | 1.5 |
| 14400 | 83 | 80 | 81.1 | 1.6 | 1.9 |

## V. CONCLUSION

We built a 3-D electrothermal model to simulate the InP-based InGaAs/GaAlAs SL microrefrigerators using ANSYS finite element analysis method. We analyzed the nonideal factors including metal/semiconductor contact resistance, side contact resistance, and substrate Joule heating. The original-designed thin-film device experimentally achieved a maximum cooling of $\sim$0.8 °C or an equivalent CPD of 135 W/cm$^2$. Our simulation results demonstrated that the optimized device with a higher SL thickness, (10 $\mu$m), reduced metal/semiconductor contact resistance, and reduced side contact resistance, could achieve a maximum cooling of 3 °C or an equivalent CPD of 195 W/cm$^2$. Furthermore, if we could introduce nonconserved lateral momentum in the SL structure by using embedded quantum dots, the optimized device could achieve a maximum cooling of 14 °C or an equivalent CPD of 910 W/cm$^2$. The COP of the actual device ranges from 0.3–0.6 depending on device sizes, but for an optimized device with nonconserved lateral momentum, the best COP could be improved as much as 4.7 for a device size of $120 \times 120$ $\mu$m$^2$. If we monolithically grow the optoelectronic device on top of the microrefrigerator, we could fully benefit all the cooling generated by the microrefrigerator. When we used two-chip fusion bonding integration model, the interface has been the bottleneck limiting microrefrigerators' ability to cool the target hot spots on optoelectronic modules. With the current 3-$\mu$m-thick Au bonding interface, only one-fourth to one-third of the cooling power could reach the hot spot: 50 W/cm$^2$ with the current optimized SL structure and 300 W/cm$^2$ with the lateral momentum nonconserved SL structure.

## REFERENCES


[1] Y. Zhang, J. Christofferson, D. Vashaee, P. Nguyen, G. Zeng, C. LaBounty, Y. Okuno, Y.-C. Chiu, J. Bowers, and A. Shakouri, "Thin film coolers for localized temperature control in optoelectronic integrated circuits," in *Proc. 53rd Electronic Components Technology Conf. (ECTC)*, New Orleans, LA, 2003, p. P312.

[2] H. B. Sequeira, "Thermoelectric properties of a Peltier cooled laser structure," Ph.D. dissertation, Univ. Delaware, Newark, DE, 1982.

[3] Y. Zhang, J. Christofferson, A. Shakouri, G. Zeng, J. Bowers, and E. Croke, "High speed localized cooling using sige superlattice microrefrigerators," in *Proc. 19th Annu. IEEE Semiconductor Thermal Measurement Management Symp.*, San Jose, CA, Mar. 2003, p. P61.

[4] S. Hava, R. G. Hunsperger, and H. B. Sequeira, "Monolithically peltier-cooled laser diodes," *J. Lightwave Technol.*, vol. LT-2, no. 2, p. 175, Apr. 1984.

[5] N. K. Dutta, T. Cella, R. L. Brown, and D. T. C. Huo, "Monolithically integrated thermoelectric controlled laser diode," *Appl. Phys. Lett.*, vol. 47, no. 3, p. P222, Aug. 1985.

[6] P. R. Berger, N. K. Dutta, K. D. Choquette, G. Hasnain, and N. Chand, "Monolithically peltier-cooled vertically-cavity surface-emitting lasers," *Appl. Phys. Lett.*, vol. 59, no. 1, p. P117, Jul. 1991.

[7] C. LaBounty, A. Shakouri, P. Abraham, and J. E. Bowers, "Two stage monolithic thin film coolers," in *Proc. ITherm'00 Conf.*, Las Vegas, NV, May 2000, p. 44.

[8] S. Hava and R. Hunsperger, "Thermoelectric properties of $Ga_{1-x}Al_xAs$," *J. Appl. Phys.*, vol. 57, no. 12, p. P5330, Jun. 1985.

[9] D. M. Rowe, Ed., *CRC Handbook of Thermoelectrics*. Boca Raton, FL: CRC, 1995.

[10] T. C. Harman, P. J. Taylor, D. L. Spears, and M. P. Walsh, "Thermoelectric quantum-dot superlattices with high $ZT$," *J. Electron. Mater.*, vol. 29, pp. L1–L4, 2000.

[11] M. S. Dresselhaus, T. Koga, X. Sun, S. B. Cronin, K. L. Wang, and W. Chen, "Low dimensional thermoelectrics," in *Proc. 16th Int. Conf. Thermoelectrics*, 1997, pp. 12–20.

[12] R. Venkatasubramanian, E. Siivola, T. Colpitts, and B. O'Quinn, "Thin-film thermoelectric devices with high room-temperature figures of merit," *Nature*, vol. 413, pp. 597–602, 2001.

[13] X. Fan, G. Zeng, C. LaBounty, E. Croke, D. Vashaee, A. Shakouri, C. Ahn, and J. E. Bowers, "High cooling power density SiGe/Si micro coolers," *Electron. Lett.*, vol. 37, no. 2, p. 126, Jan. 18, 2001.

[14] C. LaBounty, A. Shakouri, P. Abraham, and J. Bowers, "Monolithic integration of thin-film coolers with optoelectronic devices," *Opt. Eng.*, vol. 39, no. 11, p. 284, 2001.

[15] Y. Zhang *et al.*, "Thin film coolers for localized temperature control in optoelectronic integrated circuits," in *Proc. 53rd Electronic Components Technology Conf. (ECTC'03)*, New Orleans, LA, May 27–30th, 2003, p. P312.

[16] C. LaBounty, A. Karim, X. Fan, G. Zeng, P. Abraham, Y. Okuno, J. E. Bowers, J. Christofferson, D. Vashaee, A. Fitting, A. Shakouri, and E. Croke, "Wafer-fused thin film cooler semiconductor laser structures," in *Proc. 20th ICT'01 Conf.*, Jun. 2001, p. P397.

[17] B. Yang and G. Chen, "Partially coherent phonon heat conduction in superlattices," *Phys. Rev. B*, vol. 67, no. 195 311, 2003.

[18] J. Zhang, N. G. Anderson, and K. M. Lau, "AlGaAs superlattice microcoolers," *Appl. Phys. Lett.*, vol. 83, no. 2, p. P374, Jul. 2003.

[19] G. Chen, M. S. Dresselhaus, G. Dresselhaus, J.-P. Fleurial, and T. Caillat, "Recent developments in thermoelectric materials," *Int. Mater. Rev.*, vol. 48, no. 1, 2003.

[20] "ANSYS Release no. 7.0," ANSYS, Inc., Canonsburg, PA, 2003.

[21] S. T. Huxtable, C. LaBounty, A. Shakouri, P. Abraham, Y.-J. Chiu, X. Fan, J. E. Bowers, and A. Majumdar, "Thermal conductivity of InP-based superlattices," *Microsc. Thermophys. Eng.*, vol. 4, no. 3, p. 594, 2000.

[22] Y. Zhang, G. Zeng, R. Singh, J. Christofferson, E. Croke, J. E. Bowers, and A. Shakouri, "Measurement of seebeck coefficient perpendicular to SiGe superlattice," in *Proc. 21st ICT'02 Conf.*, Long Beach, CA, Aug. 2002, p. 329.

[23] Y. Zhang *et al.*, "3-D electrothermal simulation of heterostructure thin film microcooler," in *Proc. ASME Symp. Analysis Applications Heat Pump Refrigeration Systems*, Washington, DC, Nov. 16–21, 2003.

[24] Y. Zhang, D. Vashaee, R. Singh, G. Zeng, and A. Shakouri, "Influence of doping concentration and ambient temperature on the cross-plane seebeck coefficient of InGaAs/InAlAs superlattices," in *Proc. Materials Research Soc. Symp.*, Boston, MA, Dec. 1–5, 2003, p. 59.

[25] D. Vashaee and A. Shakouri, "Improved thermoelectric power factor is metallic-based superlattices," *Phys. Rev. Lett.*, vol. 92, no. 10, Mar. 12, 2004. 106 103.

[26] ——, "Conservation of lateral momentum in heterostructure integrated thermionic coolers," in *Proc. Materials Research Soc. Symp.*, vol. 691, Boston, MA, Nov. 2001, pp. 131–145.

[27] C. LaBounty, D. Oberle, J. Piprek, P. Abraham, A. Shakouri, and J. E. Bowers, "Monolithic integration of solid state thermionic coolers with semiconductor lasers," in *Proc. Laser Electro Optics Soc. Annu. Meeting (LEOS)*, Nov. 2000.

[28] G. L. Solbrekken, Y. Zhang, A. Bar-Cohen, and A. Shakouri, "Use of superlattice thermionic emission for "hot spot" reduction in a convectively-cooled chip," in *Proc. Itherm'04*, Las Vegas, NV, Jun. 1–4, 2004, p. 610.

**Yan Zhang** received the B.S. degree from Shanghai University, Shanghai, China, in 1997 and the M.Sc. degree from the National University of Singapore in 1997. She is currently pursuing the Ph.D. degree at the Electrical Engineering Department, University of California, Santa Cruz.

Her current research is on nano-scale heat and current transport in semiconductor devices, utilizing microrefrigerator for on-chip cooling solution and electrothermal energy conversion.

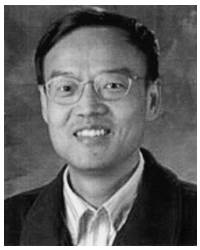

**Gehong Zeng** received the B.S. degree from the South China Institute of Technology, Guangzhou, in 1982 and the M.S. and Ph.D. degrees from Shaanxi Microelectronics Research Institute, Xian, China, in 1987 and 1992, repectively.

He was with the Kunming Institute of Physics, Kunming, China, working on infrared detectors and imagers. He is currently with the Electrical and Computer Engineering Department, University of California, Santa Barbara. His research interests include design, fabrication, and testing of optoelectronic devices.

**Joachim Piprek** received the Ph.D. degree in solid state physics from Humboldt University, Berlin, Germany.

Both in industry and in academia, he worked on semiconductor and optoelectronic device physics and simulation. He is currently an Adjunct Associate Professor with the University of California, Santa Barbara. He published more than 100 technical papers, four book chapters, and two books.

Dr. Piprek founded and Co-Chairs the annual NUSOD Conference.

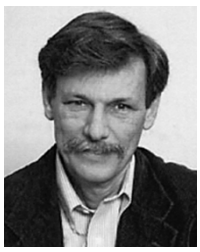

**Avram Bar-Cohen** (M'85–SM'87–F'93) received the B.S. (with honors) and M.S. degrees, and the Ph.D. degree, from the Massachusetts Institute of Technology, Cambridge, in 1968 and 1971, respectively, all in mechanical engineering.

He is Professor and Chair of Mechanical Engineering at the University of Maryland, College Park, where he continues his research in the thermal management of Micro/Nano systems. He began his professional career at the Raytheon Company in Massachusetts in 1968 and for the past 35 years has been involved in the design, analysis, and optimization of thermal systems, with emphasis on the thermal packaging of electronic equipment. He has lectured widely, published extensively in the archival heat transfer and packaging literature, and taught many short courses on this subject, at universities and major conferences in the U.S. and abroad. He served as General Manager and Executive Consultant for packaging and physical modeling at Control Data Corporation, from 1984 to 1989, held a succession of academic appointments, from Lecturer to Professor, in the Department of Mechanical Engineering, Ben Gurion University of the Negev, Israel, from 1973 to 1988, and was on the faculty at the Massachusetts Institute of Technology, from 1977 to 1978, and the Naval Postgraduate School, in1982. He is coauthor of *Design and Analysis of Heat Sinks* (New York: Wiley, 1995) and *Thermal Analysis and Control of Electronic Equipment* (New York: McGraw-Hill/Hemisphere, 1983), and has coedited 13 books in this field, including the ASME Press Series *Advances in Thermal Modeling of Electronic Components and Systems* and the series *Thermal Management of Microelectronic and Electronic Systems* (New York: Wiley). He has authored and coauthored some 250 journal papers, refereed proceedings papers, and chapters in books, and has delivered nearly 50 Keynote, Plenary, and Invited Lectures at major technical Conferences and Institutions. He served as the ASME Vice President for Research (1998-2001) and had earlier served on ASME's Board of Research and Technology Development, as well as the ASME Board on Professional Development, and was instrumental in reviving the HTD K-16 Committee on Heat Transfer in Electronic Components in the early 1980's. He was a founding member and currently serves on the Advisory Board of ASME's Nanotechnology Institute and represents ASME on the Assembly for International Heat Transfer Conferences (2002 to 2006). Prior to accepting his current position, he served as the Director of the Center for the Development of Technological Leadership and held the Sweatt Chair at the University of Minnesota, where he earlier served as Professor of Mechanical Engineering and Director of the Thermodynamics and Heat Transfer Division. His interests include thermal design, ebullient heat transfer, and thermal phenomena in microelectronic, photonic, and biological systems, as well as technology forecasting and management of technology.

Dr. Bar-Cohen received the 2001 IEEE CPMT Society Outstanding Sustained Technical Contributions Award, the 2000 ASME Worcester Reed Warner Medal, the ASME Heat Transfer Memorial Award, the ASME Curriculum Innovation Award in 1999, the ASME/IEEE ITHERM Achievement Award in 1998, the ASME Edwin F. Church Medal in 1994, and the THERMI Award from the IEEE/Semi-Therm Conference in 1997. He is a Fellow of ASME, the Editor-in-Chief of the IEEE TRANSACTIONS ON COMPONENTS AND PACKAGING TECHNOLOGIES, a Distinguished Lecturer for IEEE, was the Founding Chairman of the ITHERM Conference in 1988, and served as the General Chairman for the first InterPack Conference in 1995.

**Ali Shakouri** received the M.S.E.E. degree from Ecole Nationale Superieure des Telecommunications, Paris, France, in 1990 and the Ph.D. degree from the California Institute of Technology, Pasadena, in 1995.

He is Associate Professor of electrical engineering at the University of California, Santa Cruz. He is currently the Director of the Thermionic Energy Conversion Center (a multiuniversity research initiative aiming to improve direct thermal to electric energy conversion technologies). His current research is on nanoscale heat and current transport in semiconductor devices, submicron thermal imaging, micro refrigerators on a chip and novel optoelectronic integrated circuits.

Dr. Shakouri received the Packard Fellowship in 1999 and the NSF CAREER Award in 2000.